Water Transport Mechanisms through Asymmetric Membranes

E. G. CERRELLA and H. A. MASSALDI, *Instituto Multidisciplinario de Biología Celular (IMBICE), C. Correo 403, La Plata, Argentina*

Synopsis

Permeability coefficients and activation energy values for the transport of water through asymmetric cellulose acetate membranes were determined in order to establish the mechanism of the process when different driving forces are applied. A stirred Lucite cell with controlled temperature was used to measure the membrane transport properties under hydraulic and osmotic pressure differences and also in the presence of a tracer concentration gradient across the membrane. The experimental results based on the temperature dependence of water flow show that the controlling step for water transport is diffusion with net flux in the dense zone of the membrane under hydraulic or osmotic pressure gradients. When a tracer concentration gradient is used, equimolar diffusion of water in the thicker, porous zone of the membrane is the controlling mechanism. A mass transport model based on the composed structure of the membrane is presented to provide a general framework for treating the particular cases. Finally, the difference in the controlling barriers, in agreement with a previous work by Hays,[18] is shown to account for the much higher absolute values of osmotic than tracer water permeabilities determined here and frequently reported in the literature.

INTRODUCTION

Water transport through membranes is an essential feature of numerous biological processes, where the absorption or elimination of water contributes to the self-regulation of living organisms. Also, recently developed industrial operations, such as reverse osmosis and ultrafiltration, depend on the water transport velocity through synthetic membranes to become competitive with other separation processes.[1] However, owing to the inherent complex structure of membranes, the mechanism of water transport is still not clearly understood, and various models and theories have been proposed to explain the large differences in permeability observed when osmotic—or hydraulic—and tracer experiments are carried out.[2-4]

Among these, water transport by essentially viscous flow through existing pores in the membrane has been invoked for the osmotic experiments, whereas equimolar diffusion of labeled water through the same pores would be the relevant mechanism in the tracer experiments.[5-7] In this way, the generally much higher values of osmotic permeabilities with respect to the tracer permeabilities are accounted for and allow the calculation of an "equivalent pore radius" of the membrane.[3,7,8]

However, various experimental and theoretical objections have been pointed out with respect to the general application of the pore model to selective membranes. Thus, similar results have been obtained with membranes apparently devoid of pores.[9,10] Also, selectivity by a steric effect cannot be sustained since molecular size is not the only parameter followed in the exclusions of solutes from the membrane.[7] Among the theoretical objections, the difficulty in assuming

Journal of Applied Polymer Science, Vol. 26, 1243–1256 (1981)
 CCC 0021-8995/81/041243-14$01.40

the validity of the Poiseuille law or a simple modification of it, in the limit of the small radii derived from the calculations,[11,12] may be mentioned. There is also the resistance of the unstirred boundary layers, first pointed out by Dainty,[13] as being responsible for lower values of the tracer permeability, the osmotic permeability being only moderately affected; and finally the fact that a higher osmotic than tracer permeability is predicted by the diffusional model if the frame of reference correction for net flow is considered.[11,14–16] This means that bulk flow does not necessarily imply viscous flow,[17] and for this case, the polymeric or "inert" structure of the membrane must be considered as a component of the phase. Those authors recognize, however, that this correction cannot explain the order of magnitude difference encountered in several biological membranes, where the volume fraction of water is low.

Interestingly, Hays,[18] in connection with the mechanism of vasopressin action, had previously presented a feasible explanation to this problem, on the basis of different controlling barriers—consisting of a series of narrow and wide pores—to osmotic and tracer water flow, that might exist in some types of biological membranes. However, the mechanism of osmotic flow still remains obscure, since the assumption is made of the existence of molecular size pores, to which the criticism mentioned above is appliable.

Superimposed on all this, there is a great deal of confusion in the available data, arising both from difficulties in performing precise measurements, particularly in biological membranes, and several ill definitions in the permeabilities and driving forces used.[16,19]

The present work was undertaken with the purpose of (1) developing a general model for water transport in a bilayer asymmetric membrane and (2) to ascertaining what the mechanism for osmotic flow is in the corresponding controlling barrier of the membrane.

Water transport is measured through a reverse osmosis membrane, under different driving forces, and the permeability and activation energy of the processes are obtained and compared on the basis of the membrane structure and the relevant transport equations.

EXPERIMENTAL

Method

Cell Used in Permeability Measurements

Figure 1 illustrates the cell assembly, which consists of a membrane clamped and sealed with O-rings between a set of 40-mm-i.d. symmetrical Lucite cells, 70 mm long. Stirring shafts enter horizontally through the outer ends of the cell. Both compartments are surrounded by thermostatization jackets. Temperature is measured by copper–Constantan thermocouples located in the center of each cell. During the osmotic and hydraulic experiments, water volume flow is measured by means of calibrated capillaries attached to the chambers and half-filled with the solution corresponding to each one.

The pressure difference in the chambers is achieved by changing the height of the reservoir that feeds one of the compartments.

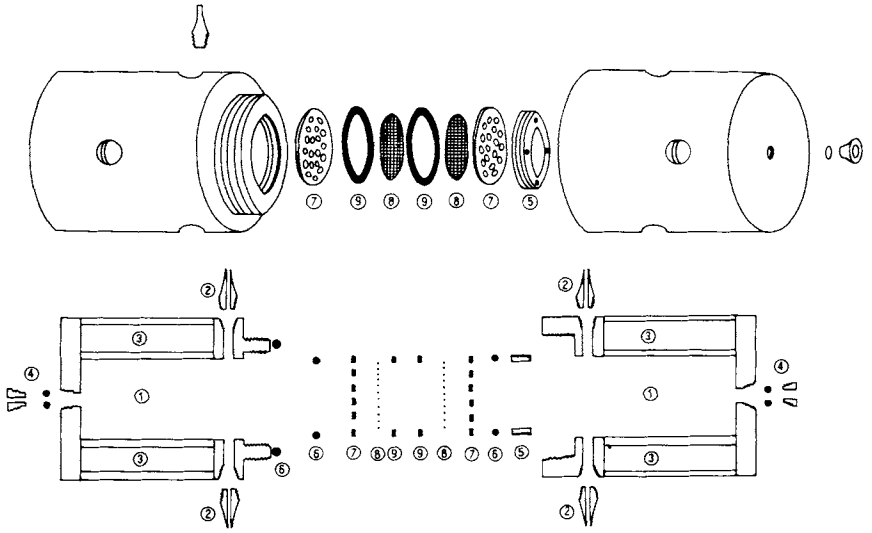

Fig. 1. Transverse section of the cell used for permeability measurements: (1) hemicell, (2) feed and purge valves, (3) thermostatization jacket, (4) hollow lid and O-ring, (5) screw part, (6) O-rings, (7) perforated brass plates, (8) plastic mesh disks, (9) rubber seals.

The Membrane

The synthetic membrane used, purchased from De Danke Sukkerfabrikker Drifternisk Laboratorius, No. 985, was made of cellulose acetate of the type used in reverse osmosis processes. It was selected because of its great selectivity (high rejection of solutes) and relatively high water flow, which resembles the behavior of biological membranes to water transport.

These membranes are known to consist of a thin, dense layer (0.2 μm thick) over a thicker, highly swollen open-pore structure (50 μm thick). Their high selectivity is attributed mainly to the relatively dense surface layer.[20]

Experimental Procedure

Hydraulic Measurements

The cells were filled with distilled water and purged of air bubbles. After constant temperature was achieved, the valves were closed and pressure differences were established so as to measure menisci displacements either forward or backward in the capillaries. Only steady-state values were considered, when the menisci moved linearly, at constant velocity.

Osmotic Measurements

The cells were filled with aqueous solutions of different solute concentrations on one side of the membrane and water on the other side. The aqueous solutions used were (1) Cl_2Ca (0.1%): samples were taken from both compartments at the beginning and at the end of the experiments; they were analyzed by Mohr's method. The membrane rejection to Cl_2Ca was in the order of 95%. (2) Sucrose: the working concentrations were in the range of (1–3) $\times 10^{-3}$ mole/l; the membrane rejection to sucrose was 100%, within the sensibility of the method.

The solutions were in contact with the dense layer side of the membrane. An adequate stirring speed was used in order to attain constant water flow. Only the solution side was stirred and the volume flow was measured in the capillary attached to the pure water compartment, so that vibrations or air bubbles introduced by the stirrer had no effect on the readings. The runs were done with the valves open to the atmosphere and equal level of liquid in both chambers. The experiments were repeated at different temperatures and for several membranes.

Isotopic Measurements

Experiments were carried out with ordinary water on one side and tritiated water on the other side of the membrane. In this case both compartments were stirred and higher stirring speeds were needed. These experimental conditions brought about several problems which led to less reliable results. Samples were taken from both chambers at 10-min intervals and were mixed with scintillator liquid to be analyzed in a Packard Tri-Carb scintillation counter.

MEMBRANE STRUCTURE AND TRANSPORT MODEL

The asymmetric membrane model consists of two zones of different properties, the δ and ϵ phases, which separates two aqueous phases, α and β, as shown in Figure 2(a). The ϵ phase has a porous structure; the polymer constitutes the matrix and the liquid is filling the pores. These are wide enough to assume that the solution within them forms an isolated phase and thus the polymer becomes an inert structure.

The δ phase is a dense, homogeneous one, in which the polymer and water form a binary solution. Any solute that goes through this zone forms part of the solution and constitutes, with the water and polymer, a multicomponent system.

Transport Equations for Net Water Flux across the Membrane

Since phase δ is homogeneous and there is no solute, a binary diffusion mechanism for water is postulated, the polymer being the second component. In this case, the total water flux, measured relative to fixed coordinates, is[21]

$$N_w = J_w + C_w(\overline{V}_w N_w + \overline{V}_p N_p) \tag{1}$$

where J_w is the diffusive flux measured with respect to the average volumetric velocity and $N_p = 0$ in this system. This is equivalent to a Stephan flow[21] where the polymer is the stagnant component. We then have,

$$N_w = -D_w^\delta (dC_w/dy) + C_w \overline{V}_w N_w \tag{2}$$

By assuming $\overline{V}_w$ independent of C_w and integrating in thickness δ with N_w and D_w^δ constants, we obtain[16,17]

$$N_w = \frac{D_w^\delta}{y^\delta (1 - \varphi_w^\delta)_{ml}} (C_w^{\delta\epsilon} - C_w^{\delta\beta}) = k^\delta (C_w^{\delta\epsilon} - C_w^{\delta\beta}) \tag{3}$$

where $\varphi_w^\delta = C_w \overline{V}_w$. In phase ϵ, viscous flow is assumed as follows:

$$N_v = (nr^2/8\eta\tau y^\epsilon)\Delta p = k^\epsilon V_w \Delta p \tag{4}$$

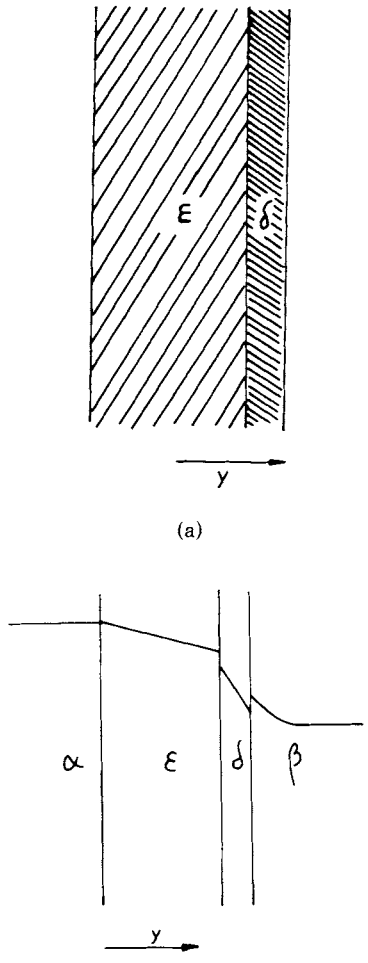

Fig. 2. (a) Schematic picture of the membrane structure. (b) Water concentration profiles across the membrane during osmosis.

Transport Equations Without Net Flux Across the Membrane

Equimolar diffusion takes place in both phases. In phase δ, the multicomponent system ordinary water, tritiated water, and polymer can be reduced to an effective binary one,[16]

$$N_w^+ = J_w^+ = (D_w^{+\delta}/y^\delta)(C_w^{+\delta\beta} - C_w^{+\delta\epsilon}) = k^{+\delta}(C_w^{+\delta\beta} - C_w^{+\delta\epsilon}) \tag{5}$$

In phase ϵ,

$$N_w^+ = (D_w^{+\epsilon}/\tau y^\epsilon)(C_w^{+\epsilon\delta} - C_w^{+\epsilon\alpha}) = k^{+\epsilon}(C_w^{+\epsilon\delta} - C_w^{+\epsilon\alpha}) \tag{6}$$

Overall Permeability

Since the phenomenon is taking place between various phases of different structural properties, it is convenient to resort to a generalized driving force, which for the transport of matter is the chemical potential.[22,23] The general expression for the chemical potential of water in a solution is

$$\mu_w = \mu_w^0 + RT \ln (\gamma_w C_w / C_w^0) + (p - p^0)\overline{V}_w \tag{7}$$

where C_w^0 is the water concentration corresponding to μ_w^0, the reference state, in this case pure water at pressure p^0 and at the temperature of the system; γ_w is water activity coefficient, and $\overline{V}_w$ is the partial molar volume of water which, as we are working with very dilute solutions, is assumed equal to the pure molar volume of water, V_w.

Hydraulic Permeability

For the hydraulic experiments, the chemical potential in each phase is, from eq. (7),

$$\mu_w^\alpha = \mu_w^0 + V_w(p^\alpha - p^0) \tag{8}$$

$$\mu_w^\beta = \mu_w^0 + V_w(p^\beta - p^0) \tag{9}$$

$$\mu_w^\epsilon = \mu_w^0 + V_w(p^{\epsilon\delta} - p^0) \tag{10}$$

$$\mu_w^\delta = \mu_w^0 + RT \ln \gamma_w^\delta (C_w^\delta / C_w^0) \tag{11}$$

From these expressions and the transport equation in phases δ and ϵ when there is net flux (eqs. (3) and (4)), the following is obtained[17]:

$$N_v = V_w N_w = P_h(p^\alpha - p^\beta) \tag{12}$$

where

$$P_h = \left[\frac{1}{k^\delta K V_w^2/RT} + \frac{1}{k^\epsilon V_w}\right]^{-1} \tag{13}$$

is the hydraulic permeability.

Osmotic Permeability

In a similar way it can be developed an expression for the osmotic permeability, but now it must be considered that there exists a solution at one side of the membrane and so an additional diffusional resistance may arise in that phase owing to boundary layer effects.

Therefore, another flux equation must be added to eqs. (3) and (4); this is[17]:

$$N_w = k^\beta(C_s^\beta - C_s^{\beta\delta}) = (k^\beta/RT)(\pi^\beta - \pi^{\beta\delta}) \tag{14}$$

assuming that the van't Hoff equation holds. C_s is the molar solute concentration.

The expressions for the flux and the osmotic permeability now are

$$N_v = V_w N_w = P_{os}\pi^\beta = P_{os}\Delta\pi \tag{15}$$

and

$$P_{os} = \left[\frac{RT}{k^\delta K V_w^2} + \frac{1}{k^\epsilon V_w} + \frac{RT}{k^\beta V_w}\right]^{-1} \tag{16}$$

Figure 2(b) shows concentration profiles for this case.

Isotopic Permeability

In this case there is no net flux across the membrane and the transport is diffusive both in phases δ and ϵ. The expression for the water tracer flux is

$$N_w^+ = P^+(C_w^{+\beta} - C_w^{+\alpha}) \tag{17}$$

where

$$P^+ = \left[\frac{1}{k^{+\delta}KV_w} + \frac{1}{k^{+\epsilon}} + \frac{2}{k^+}\right]^{-1} \tag{18}$$

is the isotopic permeability and $k^+ = k^{+\alpha} = k^{+\beta}$ represents the resistance of the external boundary layer in phases α and β.

RESULTS

Hydraulic and Osmotic Experiments

The experimental data show a linear relation between the flux across the membrane and the applied driving force (hydraulic or osmotic pressure difference), as is seen in Figure 3. From eq. (12),

$$P_h = N_v/\Delta p \tag{19}$$

Analogously, from eq. (15),

$$P_{os} = N_v/\Delta\pi \tag{20}$$

From the experimental measurements, the N_v and Δp (or $\Delta\pi$) data were obtained and by applying a least-squares regression to eqs. (19) and (20), the P_h and P_{os} values were determined at each temperature. Details are given by Cerrella.[17]

To obtain the activation energy of each process, an Arrhenius-type relationship was considered:

$$\ln P = \ln k^0 - E_a/RT \tag{21}$$

By least-squares regression of eq. (21), the values of activation energy and their confidence limits were obtained. These are shown in Table I. The plot of ln P vs. $1/T$ was linear for all cases, as shown in Figure 4.

Table II allows a comparison of the values of P_h and P_{os} obtained from these plots, corresponding to the same temperature and membrane.

Isotopic Experiments

Considering the flux defintion in phase α,

$$N_w = \frac{1}{A}\frac{dm^\alpha}{dt} = \frac{V_w^\alpha}{A}\frac{dC_w^{+\alpha}}{dt} \tag{22}$$

and eq. (17), the following is obtained:

$$\ln\left(\frac{2C_w^{+\beta} - C_{w0}^{+\beta}}{C_{w0}^{+\beta}}\right) = -\frac{2P^+At}{V_w^\alpha} \tag{23}$$

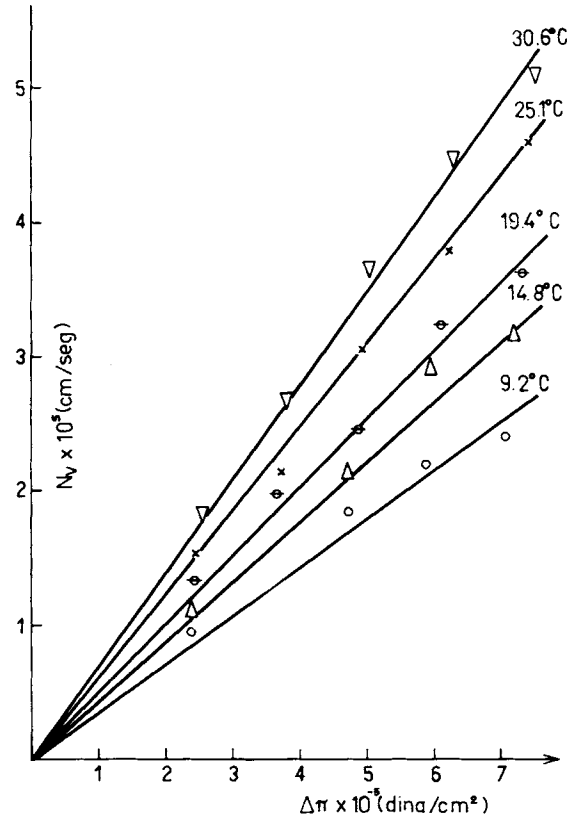

Fig. 3. Water flux vs. osmotic pressure of sucrose solutions.

By plotting ln $(2C_w^{+\beta} - C_{w0}^{+\beta}/C_{w0}^{+\beta})$ vs. t, the value of P^+ is obtained. The average value from four similar experiments was $P^+ = 5 \times 10^{-4}$ cm/sec, which must be considered only an approximate value, because of the lower precision of the measurements, already mentioned.

In Figure 5 depletion and accumulation curves are presented, in the form of the ratios $C_w^{+\alpha}/C_{w0}^+$ and $C_w^{+\beta}/C_{w0}^+$ versus time.

DISCUSSION

Equations (13), (16), and (18) include all the possible resistances and factors that can affect the value of overall water permeabilities, either osmotic, hydraulic, or tracer. Similar equations could be developed for the flux of other permeants. Thus, the permeability is clearly shown to be an overall phenomenological

TABLE I
Activation Energy Values

E_a, kcal/mole	95% Confidence limits	Driving force
5.75	±1.03	hydraulic
5.48	±1.34	osmotic (sucrose)
4.78	±1.16	osmotic (Cl_2Ca)

TABLE II
Hydraulic and Osmotic Permeability Values

T, K	$P_h \times 10^{10}$, cm / sec dyn cm^{-2}	$P_h \times 10$, cm/sec	$P_{os(CaCl_2)} \times 10^{10}$, cm / sec dyn cm^{-2}	$P_{os(sucrose)} \times 10^{10}$, cm / sec dyn cm^{-2}
283	0.5668	0.738	0.3229	0.3691
288	0.6776	0.897	0.3745	0.4374
293	0.8048	1.080	0.4321	0.5154
298	0.9507	1.303	0.4963	0.6040
303	1.1167	1.556	0.5674	0.7041

coefficient composed, among other factors, of the intrinsic permeabilities of the membrane (the k^{δ} and k^{ϵ} terms), which in turn are dependent on the properties of the different structural zones. This view is also shared by other authors.[24]

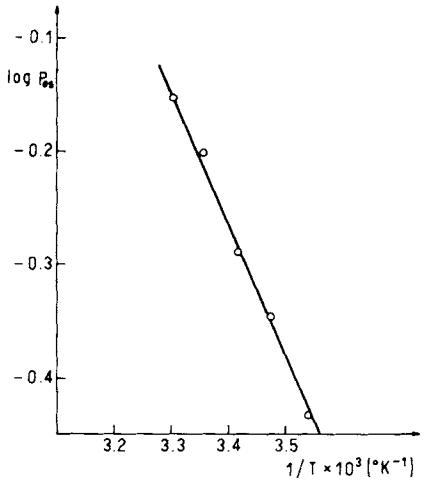

Fig. 4. Temperature dependence of osmotic permeability.

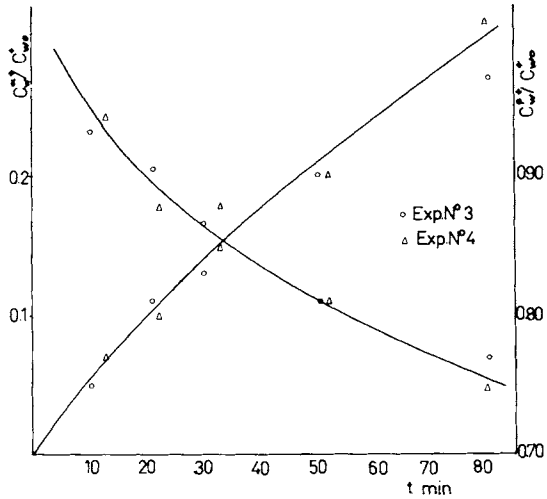

Fig. 5. Depletion and accumulation curves. Tracer experiments.

In order to establish transport mechanisms, it is customary to compare the absolute value of permeabilities obtained under different conditions. We shall first follow this approach, with careful attention given to the pertinent resistances.

Hydraulic and Osmotic Permeabilities

The linear plot shown in Figure 3 indicates that P_{os} remains constant within the concentration range explored. A similar statement is valid for the P_h plot, not shown. The values of P_{os} at 20°C (Table I) are lower than those corresponding to P_h at the same temperature, that is, P_{os} = 55 and 65% of the P_h for osmotic experiments with Cl_2Ca and sucrose, respectively. From irreversible thermodynamics, it can be shown that both permeabilities P_{os} and P_h should be the same for a strictly semipermeable membrane,[22] which is not the situation just mentioned. It may be argued that in the experiments with Cl_2Ca the assumption of semipermeability does not hold strictly, and thereby the lower value of $P_{os,(Cl_2Ca)}$ can be qualitatively explained by a decrease in the effective driving force due to migration of Cl_2Ca to the pure solvent side. This is supported by the data of membrane rejection of Cl_2Ca, which is reported to be 98%.

However, a similar trend, though less marked, is observed for the sucrose experiments, where the reported rejection is 100%, also verified experimentally. To explain this behavior, we go back to eqs. (13) and (16), which show the contributions of different resistances to the overall permeabilities.

The P_{os} term contains one additional resistance with respect to the P_h term that accounts for the presence of the external boundary layer (nonstirred layer) on the solution side, the two other resistances being the same. The effect of this layer can often be made to disappear by proper stirring, that is, when the flux becomes invariant with the stirring speed. However, in the present case, even though constant flux was reached at a moderate stirring speed, the necessary presence of the perforated disks created a stagnant zone adjacent to the membrane that could not be removed by stirring (See Fig. 6). A quantitative estimation of this effect would be difficult, however, owing to fluidodynamic complexity in the vicinity of the membrane. Its effect is similar to the "concentration polarization" effect described in connection with reverse osmosis phenomena.[20]

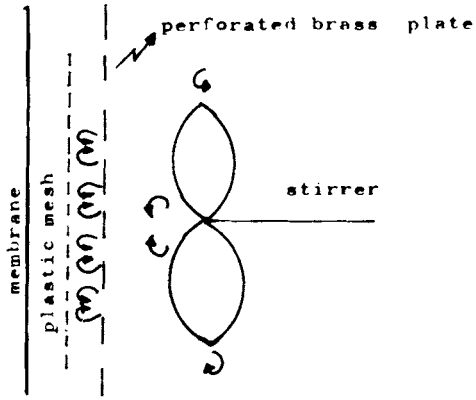

Fig. 6. Stirring effect on the membrane assembly.

Now let us consider the resistances in the membrane itself, represented by the terms $RT/k^{\delta}KV_w^2$ and $1/k^{\epsilon}V_w$, where k^{δ} is a mass transfer coefficient, defined by eq. (3), and k^{ϵ} is the intrinsic hydraulic permeability, defined by eq. (4). The value of $k^{\epsilon}V_w$ can be estimated as follows. From eq. (4),

$$k^{\epsilon}V_w = nr^2/8\eta\tau y^{\epsilon} \tag{24}$$

For a similar type of membrane, Londsdale et al.[25] found that 50% of the pores in the porous zone had a pore radius larger than 0.1 μm. In order to perform a conservative estimate, we shall assume 50% of the pores to have a radius of 0.1 μm. With this assumption it can be shown[17] that

$$n = \frac{\phi\ 0.5y^{\epsilon}\ 1\ \text{cm}^2}{r^2 \times y^{\epsilon}} \tag{25}$$

where ϕ, the porosity of the porous phase of the membrane, is about 0.7.[25,17]

Then, sustituting $\eta = 0.01$ poise, $\tau = 5$,[26] and $y^{\epsilon} = 5 \times 10^{-10}$ cm, and substituting eq. (25) into eq. (24), we obtain

$$k^{\epsilon}V_w = 1.75 \times 10^{-8}\ \text{cm/sec dyn cm}^{-2}$$

Since the highest experimental value of P_h is 1.1×10^{-10} cm sec dyn cm^2, it follows that $RT/k^{\delta}KV_w^2$ is the principal resistance in the hydraulic experiments. For the same type of membrane, Hays[18] arrived at a similar result. The same approach can be applied to the osmotic permeability (with sucrose as the solute) since the situation within the membrane is the same (water and polymer in zone δ and pure water in the pores of zone ϵ). The difference in the experimental values, however, can cast some doubt as to whether the same reasoning can be applied to both experimental situations.

Activation Energies and Transport Mechanisms

The presence of additional effects in the measurements of permeabilities under different conditions, as the one mentioned above, does not allow one to draw definite conclusions from the comparison of absolute values. For this reason, the verification of the relevant transport mechanism was confirmed by the determination of activation energies for both processes.

The values obtained, with their respective confidence limits, are

$$\begin{aligned} E_{a,h} &= 5.75 \pm 1.03\ \text{kcal/mole} \\ E_{a,os} &= 5.48 \pm 1.34\ \text{kcal/mole} \end{aligned} \tag{26}$$

It can be stated that $E_{a,h}$ and $E_{a,os}$ are estimates of the same value, that is, there exists only one activation energy for both processes. The slight difference between them may reflect the effect of the external boundary layer, the value of $E_{a,h}$ being more precise. The linearity of the plots (Fig. 4) also ensures that there is a unique mechanism in the range of temperature covered.

That this activation energy corresponds to water diffusion in zone δ can be inferred by comparing the activation energy for a purely viscous process: $E_{a,\eta}$ = 4.15 kcal/mole (obtained from data in *Handbook of Chemistry and Physics*[27]). This should have been the experimental result if the controlling mechanism were viscous flow in the pores of zone ϵ. The difference from the observed values of $E_{a,h}$ and $E_{a,os}$ is clear.

On this basis, it can be stated that diffusion of water through stagnant polymer in zone δ is the controlling mechanism, both for the hydraulic and the osmotic experiments. Viscous flow does exist in zone ϵ, but only as a consequence of the net flow generated in zone δ, and does not contribute significantly to the overall resistance. This confirms the previous approach based on comparison of absolute values and individual resistances.

Isotopic Permeability

The determination of isotopic permeability is normally performed in this kind of study as a reference value which represents an equimolar and in this case also equivolumetric, diffusive phenomenon.[28] As was already mentioned, very frequently the reported values are much lower than those corresponding to P_h or P_{os}, and it is mainly this fact that led in the early works to the pore model for membranes. The situation in this respect was not different in the present work, independently of some experimental problems that made the P^+ value less reliable than those for P_h and P_{os}. Thus, the experimental value for the tracer permeability was $P^+ = 5 \times 10^{-4}$ cm/sec at 20°C, three orders of magnitude less than those for P_h and P_{os}.

The reason for this behavior stems from a different controlling resistance when the tracer determination is carried out.[18] Thus, the isotopic permeability is determined by the diffusive properties of zone ϵ, whereas the hydraulic and osmotic permeabilities are determined by those of zone δ, with a much lower resistance than zone ϵ, in the presence of net flow. It is interesting to note that permeability results of this type have been reported for red cells,[8] which according to recent works[29] present a membrane structure similar to that of the membrane used here.

CONCLUSIONS

On the basis of a general transport model for a two-layer artificial membrane of the type used here, it has been shown that the controlling transport mechanism for water is diffusion with net flow in the dense zone, when a gradient of hydrostatic or osmotic pressure is applied as driving force. For these cases, a viscous flow of pure water does exist in the porous zone in series with the controlling diffusive flow, but only as a response to the net flow originating in the dense zone, and presents a negligible contribution to the overall resistance.

These considerations are consistent with the orders-of-magnitude higher values of the osmotic—or hydraulic—permeability with respect to the tracer permeability as determined here and generally found in the literature.

NOMENCLATURE

A	area, cm^2
C	concentration, mole/cm^3
D	diffusion coefficient, cm^2/sec
E_a	activation energy, kcal/mole
K	partition coefficient, mole/cm^3
N	flux, mole/cm^2 sec, or cm/sec

P	permeability, cm/sec or cm/sec dyn cm^2
R	gas constant, dyn cm/K mole
T	temperature, K
V	molar volume, cm^3/mole
$\overline{V}$	partial molar volume, cm^3/mole
k	mass transfer coefficient, cm/sec
m	number of moles
n	number of pores
p	pressure, dyn/cm^2
r	radius, cm
t	time, sec
y	thickness, cm
$\alpha, \beta, \delta, \epsilon$	phases
γ	activity coefficient
φ	volume fraction
ϕ	porosity
η	viscosity, poises
π	osmotic pressure, dyn/cm^2
τ	tortuosity
μ	chemical potential, cal/mole

Subscripts

h	hydraulic
os	osmotic
m	membrane
0	initial state
s	solute
ml	logarithmic mean
v	water, volumetric
w	water, mass
+	water labeled

Superscripts

0	reference state

The financial support of CONICET, Argentina, is gratefully acknowledged.

References

1. C. J. King, *Separation Processes*, McGraw-Hill. New York, 1971.
2. D. A. T. Dick, *Cell Water*, Butterworths, Washington, D.C., 1966.
3. W. Stein, *The Movement of Molecules Across Cell Membranes*, Academic, New York, 1972.
4. H. Davson and J. F. Danelli, *The Permeability of Natural Membranes*, Hafner, Darien, CT, 1970.
5. D. M. Prescott and E. Zeuthen, *Acta Physiol. Scand.*, **28,** 77 (1953).
6. R. P. Durbin, H. Frank, and A. K. Solomon, *J. Gen. Physiol.*, **39,** 535 (1956).
7. C. V. Paganelli and A. K. Solomon, *J. Gen. Physiol.*, **41,** 259 (1957).
8. D. A. Goldstein and A. K. Solomon, *J. Gen. Physiol.*, **44,** (1960).
9. G. Thau, R. Bloch, and O. Kedem, *Desalination*, **1,** 129 (1966).
10. V. Sidel and J. F. Hoffman, *Fed. Proc.*, **20,** 136 (1961).
11. E. N. Lightfoot, *Transport Phenomena and Living Systems*, Wiley, New York, 1974.
12. R. I. Macey, in *Membrane Transport in Biology*, Vol. II, G. Giebisch, D. C. Tosteson, H. H. Ussing, Eds., Springer-Verlag, Berlin, 1978, Chap. 1.
13. J. Dainty, *Adv. Bot. Res.*, **1,** 279 (1963).
14. I. J. Fenichel and S. B. Horowitz, *J. Phys. Chem.*, **74,** 2966 (1970).
15. D. R. Paul, *J. Polym. Sci.*, **11,** 289 (1973).
16. E. G. Cerrella, F. Menegalli, and H. A. Massaldi, *Rev. Latinoam. Ing. Quim. Quim. Apl.*, **6,** 171 (1976).
17. E. G. Cerrella, Doctoral thesis, Facultad de Ciencias Exactas, Universidad Nacional de La Plata, La Plata, Argentina, 1979.

18. R. M. Hays, *J. Gen. Physiol.*, **51,** 385 (1968).
19. E. Rotstein and A. R. Cornish, *J. Food Sci.*, **43,** 926 (1978).
20. U. Merten, Ed., *Desalination by Reverse Osmosis*, M.I.T. Press, Cambridge, MA, 1969.
21. T. K. Sherwood, R. L. Pigford, and C. R. Wilke, *Mass Transfer*, McGraw–Hill, New York, 1975.
22. A. Katchalsky and P. Curran, *Nonequilibrium Thermodynamics in Biophysics*, Harvard Univ. Press, Cambridge, MA, 1967.
23. S. R. De Groot and P. Mazur, *Nonequilibrium Thermodynamics*, North-Holland, Amsterdam, 1969.
24. S. T. Hwang and K. Kammermeyer, *Polym. Sci. Technol.*, **6,** 197 (1974).
25. H. K. Londsdale, U. Merten, and R. L. Riley, *J. Appl. Polym. Sci.*, **9,** 1341 (1965).
26. B. Z. Ginzburg and A. Katchalsky, *J. Gen. Physiol.*, **47,** 403 (1963).
27. *Handbook of Chemistry and Physics*, 53rd ed., R. C. Weast, Ed., CRC Press, Cleveland, OH, 1973.
28. R. B. Bird, W. E. Stewart, and E. N. Lightfoot, *Transport Phenomena* Wiley, New York, 1960.
29. E. Evans and R. M. Hochmuth, *J. Membrane Biol.*, **30,** 351 (1977).

Received July 7, 1980
Accepted August 11, 1980